Int. J. Electrochem. Sci., 8 **(2013)** 490 - 503

International Journal of
ELECTROCHEMICAL
SCIENCE
www.electrochemsci.org

Copper (II) Oxide Phosphate Superstructures: Their Primarily Application as Effective Antimicrobial Materials

Guoyan Zhao[1], *Huan Pang* [1, 2, 3,*], *Huiyun Li*[1], *Juan Li*[1], *Bo Yan*[1], *Yahui Ma*[1], *Guochang Li*[1], *Jing Chen*[1], *Jianshan Zhang*[1] *and Honghe Zheng* [2*]

[1] College of Chemistry and Chemical Engineering, Anyang Normal University, Anyang, 455000 Henan, P. R. China.
[2] School of Energy, Soochow University, Suzhou, 215006, Jiangsu, P. R. China.
[3] State Key Laboratory of Coordination Chemistry, Nanjing University, Nanjing, 210093, Jiangsu, P. R. China.
[*]E-mail: huanpangchem@hotmail.com; hhzheng@suda.edu.cn;

Received: 11 October 2012 / *Accepted:* 15 November 2012 / *Published:* 1 January 2013

Copper (II) oxide phosphate ($Cu_4O(PO_4)_2$) superstructures (oblong walnut-like, screwy cubic-like, octahedron-like, rod-like, double-flower-like and so on) have been successfully synthesized by calcinations of $Cu_2(OH)PO_4$ superstructures at 600 ^oC in air. $Cu_2(OH)PO_4$ superstructures have been easily synthesized by a simple hydrothermal condition, which has been used as the precursor and followed to form $Cu_4O(PO_4)_2$ superstructures. The whole process is quite simple and easy to control by changing reaction conditions. More importantly, we have primarily studied the antibacterial properties of $Cu_4O(PO_4)_2$ superstructures. The antibacterial measurements indicate different morphologies of $Cu_4O(PO_4)_2$ superstructures with different antibacterial properties, and the bacteriostatics towards some bacteria could be used as effectively as penicillin or kanamycin.

Keywords: Copper oxide phosphate; Superstructure; Antibacterial

1. INTRODUCTION

Recently, efforts have been devoted to self-assembly of nanostructures-nanorods, nanoplates, and nanospheres in two-dimensional (2D) and three-dimensional (3D) ordered superstructures and several hierarchical architectures due to their interesting properties of such superstructures and their potential applications in many fields, including catalysis, [1] optoelectronics, [2] lithium-ion batteries, [3-5] supercapacitor [6-8], drug delivery system, [9] sensors [10, 11] and antibacterial agent. [12, 13] However, methods to manipulation of these superstructures often use solid templates, which have to be removed after the reaction, [14-16] but impurities can be introduced from the solid templates that can

affect the properties adversely. Therefore, there is a significant interest in developing spontaneous generation of novel patterns with tailored structures and shapes by facile, hard template-free, solution-based, morphology controlled approaches to building novel self-generated architectures.

Inorganic nanomaterials have been emerging as a new kind of antimicrobial materials to fulfill the increasing general demands for hygiene in daily life because of their large specific surface area and high bioactivity. The predominant antimicrobial activity of inorganic nanomaterials can be attributed to the strong cytotoxicity to various bacterial cells, i.e., they can interact with the functional groups on the bacterial cell surface and inactivate bacteria. [17–20] Nano-micromaterials generally show many size- and shape-dependent properties which are interesting for device applications, [21-30] particularly three-dimensional (3D) superstructures, in order to find potential applications in nanodevices.[31-34] However, there are nearly no reports about shapes effecting on the antimicrobial activity of 3D superstructures.

Metal phosphates have many promising applications in various areas, such as catalysis, ion exchange, proton conductivity, intercalation chemistry, photochemistry, and chemistry materials.[35-50] Copper (II) oxide phosphate, $Cu_4O(PO_4)_2$, was reported in 1978 by J. B. Anderson and Brunel-Laugt, [40, 41] but there were nearly no reports about it in the past years. [42, 43] Recently, it has been reported for the first time that $Cu_2(OH)PO_4$ with complex morphologies could be formed by hydrothermal synthesis [50]. Herein, we have successfully synthesized various $Cu_4O(PO_4)_2$ superstructures with effective antimicrobial by calcinations of $Cu_2(OH)PO_4$ superstructures at 600 ^oC in the air. The precursor $Cu_2(OH)PO_4$ superstructures have been easily synthesized by a mild hydrothermal condition. The whole process is hard template-free and very easy to control by changing different additives. What's more, different $Cu_4O(PO_4)_2$ superstructures show different antibacterial properties and the bacteriostatics towards some bacteria can be used as effectively as penicillin or kanamycin. In this regard, the following two points are desirable and significant for this study: (i) development of a facile solution based route for fabrication of high-quality $Cu_4O(PO_4)_2$ superstructures and (ii) discovery of significant antimicrobial $Cu_4O(PO_4)_2$ superstructures. While the first complements and enriches the known synthetic methods for the fabrication of superstructures, the latter provides experimental support for scientists to find potential novel applications of nano-micromaterials in the field of biomaterials.

2. EXPERIMENT

2.1 Synthesis of $Cu_2(OH)PO_4$ and $Cu_4O(PO_4)_2$ superstructures

$Cu_2(OH)PO_4$ superstructures:

S1: 0.210 g of $CuSO_4 \cdot 5H_2O$ and 0.300 g of $(NH_4)_2HPO_4$ in a solvent of 20 mL H_2O at 160 ^oC for 24 h;

S2: 0.210 g of $CuSO_4 \cdot 5H_2O$, 0.300 g of $(NH_4)_2HPO_4$ and 0.050 g of sodium dodecylbenzene sulfonate in 30 mL H_2O at 200 ^oC for 24 h;

S3: 0.210g of $CuSO_4 \cdot 5H_2O$ and 0.300 g of $(NH_4)_2HPO_4$ in a solvent of 10 mL H_2O at 200 ^oC for 24 h;

S4: 0.050 g sodium dodecylbenzene sulfonate, and other conditions are the same as S3;

S5: 0.210 g of $CuSO_4 \cdot 5H_2O$ and 0.210 g of $(NH_4)_2HPO_4$ in a solvent of 10 mL H_2O at 200 ^oC for 24 h;

S6: When increasing the reaction time to 48 hours, and other conditions are the same as S5;

S7: We have added 0.013 g sodium dodecylbenzene sulfonate, and decrease the amount of $CuSO_4 \cdot 5H_2O$ to 0.124g based on S6;

S8: 0.210 g of $CuSO_4 \cdot 5H_2O$, 0.210 g of $(NH_4)_2HPO_4$ and 0.015 g of sodium dodecylbenzene sulfonate in a solvent of 30 mL H_2O at 200 ^oC for 24 h.

$Cu_4O(PO_4)_2$ superstructures:

$Cu_4O(PO_4)_2$ superstructure can be easily obtained by calcining $Cu_2(OH)PO_4$ superstructures at 600 ^oC for 12 hours in the air at a heating rate of 1 $^oC\ min^{-1}$. After calcinations, the products obtained were named P1-P8 corresponding: S1 named P1; S2 named P2; S3 named P3; S4 named P4; S5 named P5; S6 named P6; S7 named P7; S8 named P8.

2.2 Antimicrobial measurements

The antibacterial activity of the synthesized nanostructures was tested against *B. subtilis*, *S. aureus*, *S. faecalis*, *P. aeruginosa*, and *E. cloacae* by determining the MICs (minimum inhibitory concentrations, μg/mL) through a colorimetric method using the dye MTT (3-(4,5)-dimethylthiahiazo(-z-y1)-3,5-diphenytetrazoliumromide). A stock solution of the synthesized nanosystems (50 μg mL^{-1}) was prepared in dimethyl sulfoxide (DMSO) and graded quantities of the test nanostructures were incorporated in specified quantity of sterilized liquid medium. Then the solutions were poured into microtitration plates and suspension of the microorganism with an approximate concentration of 10^5 cfu/mL was added. After incubation at 37 ^oC for 24 h, 50 μL of PBS (Phosphate Buffered Saline 0.01 mol/L, pH 7.4 : $Na_2HPO_4 \cdot 12H_2O$ 2.9 g, KH_2PO_4 0.2 g, NaCl 8.0 g, KCl 0.2 g, distilled water 1000 mL) containing 2 mg/mL of MTT was added to each well. Incubation was continued at room temperature for 4~5 h, followed by the addition of 100 μL of isopropanol containing 5 % 1 mol/L HCl to extract the dye. At last, the optical density (OD) was measured with a microplate reader at 570 nm to determine the MICs.

2.3 Characterization

To study the phase structure of the samples, X-ray diffraction (XRD) patterns were recorded by a D8 diffraction in the 2θ range of 10-70^o by using a Rigaku Ultima III X-ray diffraction with Cu-Ka radiation (λ= 0.1541 nm). Nitrogen adsorption-desorption measurements were performed on a Gemini VII 2390 Analyzer at 77 K by using the volumetric method. The specific surface area was obtained from the N_2 adsorption-desorption isotherms and was calculated by the Brunauer-Emmett-Teller (BET)

method. The morphologies and microstructures of the samples were studied by a JEOL JSM-6701F field emission scanning electron microscopy (FESEM) operating at 5.0 KV in high vacuum.

3. RESULTS AND DISCUSSION

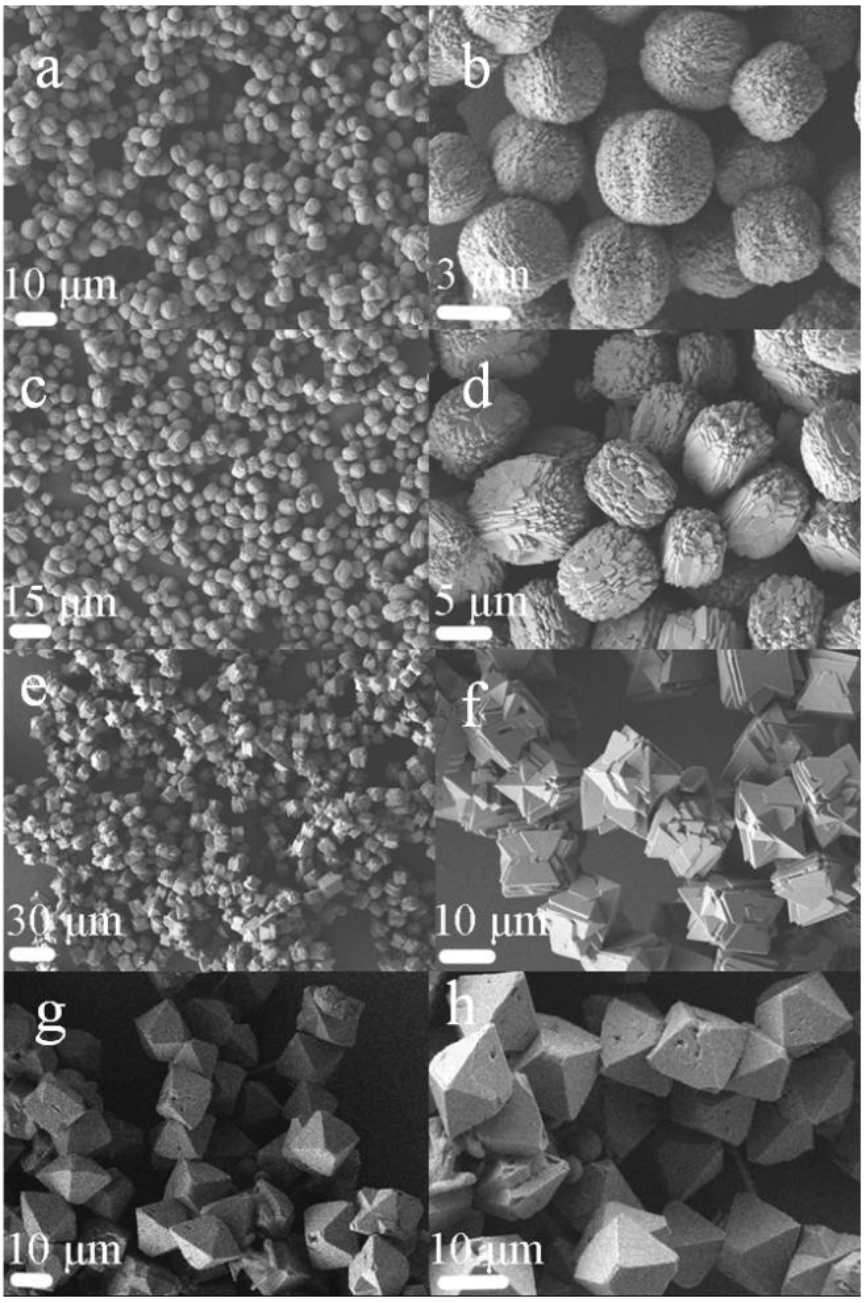

Figure 1. Typical SEM images of $Cu_2(OH)PO_4$ superstructures (a-b) S1; (c-d) S2; (e-f) S3; (g-h) S4.

ESI Fig. 1 shows a schematic crystal structure of the $Cu_2(OH)PO_4$ super cell (2×2×2 slabs) projected by a software-*Diamond 3* based on Inorganic Crystal Structure Data # 15833. $Cu_2(OH)PO_4$ has an orthorhombic crystal structure, which consists of a PO_4 tetrahedron, a $Cu(1)O_6$

octahedron, a $Cu(2)O_5$ trigonal bipyramid, and an OH group between the two Cu species. The $Cu_2(OH)PO_4$ superstructures were obtained under different hydrothermal conditions. XRD patterns in ESI Fig. 2, 3 (Electronic Supplementary Information) confirm all the products are the $Cu_2(OH)PO_4$ complexes (JCPDS No. 36-0404).

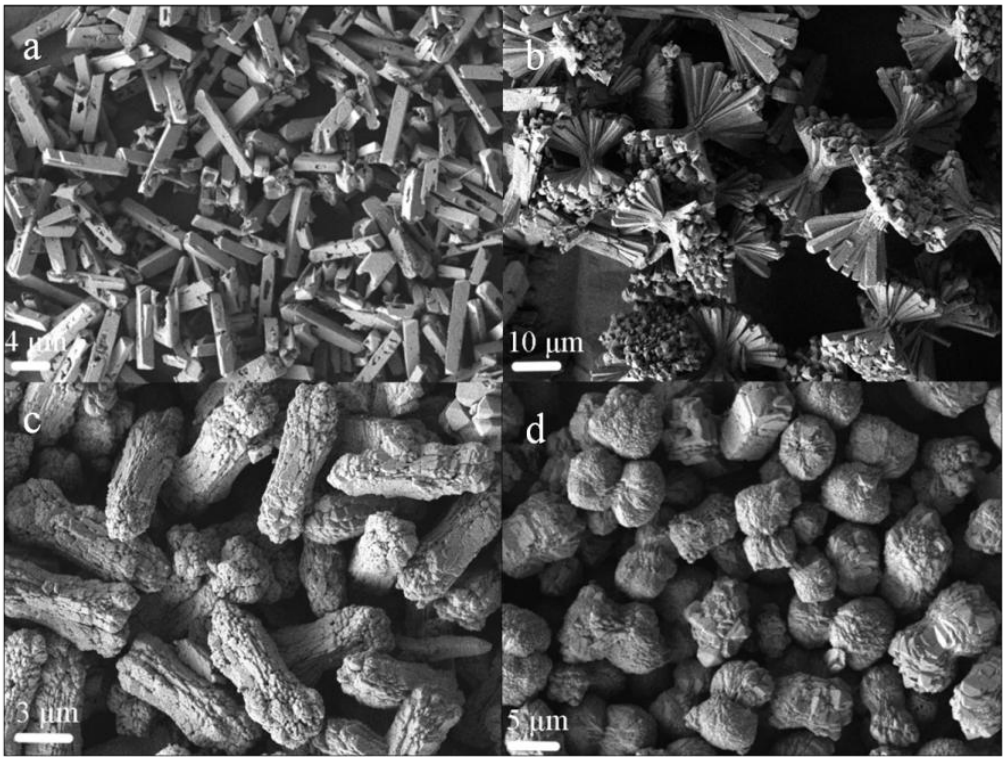

Figure 2. Typical SEM images of $Cu_2(OH)PO_4$ superstructures (a) S5; (b) S6; (c) S7; (d) S8.

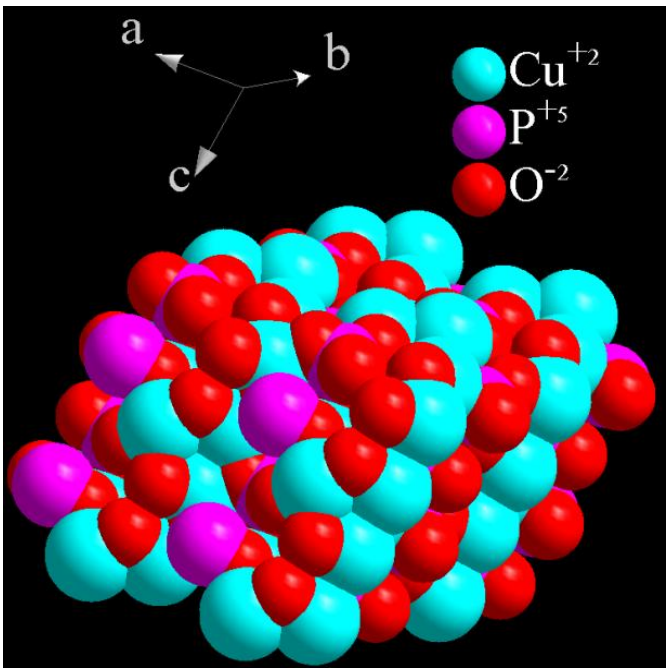

Figure 3. Crystal structure of the $Cu_4O(PO_4)_2$ super cell (2×2×2 slabs).

Fig. 1a, b display typical SEM images of the product prepared with 0.210 g of $CuSO_4 \cdot 5H_2O$ and 0.300 g of $(NH_4)_2HPO_4$ in a solvent of 20 mL H_2O at 160 ^oC for 24 h. From the image in Fig. 1a (the product named S1), it could easily be seen that the product is composed of sphere walnut-like superstructure with a size of 3-4 μm. The high magnification image in Fig. 1b clearly shows that the sphere walnut-like superstructure is made up of many nanocrystals. Fig. 1c-d (the product named S2) show SEM images of the product which was prepared with 0.210 g of $CuSO_4 \cdot 5H_2O$, 0.300 g of $(NH_4)_2HPO_4$ and 0.050 g of sodium dodecylbenzene sulfonate in 30 mL H_2O at 200 ^oC for 24 h. From the image in Fig. 1c, the product is composed of oblong walnut-like superstructure with a size of 7-8 μm. The high magnification image in Fig. 1d clearly shows that the oblong walnut-like superstructure is made up of many polygonal nanocrystals, and these polygonal particles have larger size than that of the one in Fig. 1a-b, which would probably be due to the using of sodium dodecylbenzene sulfonate which assisted nanocrystal formed in Fig. 1d. SEM images of Fig. 1e–f display typical product (the product named S3) which was prepared with 0.210g of $CuSO_4 \cdot 5H_2O$ and 0.300 g of $(NH_4)_2HPO_4$ in a solvent of 10 mL H_2O at 200 ^oC for 24 h, in which we have decreased the volume of H_2O to 10 mL.

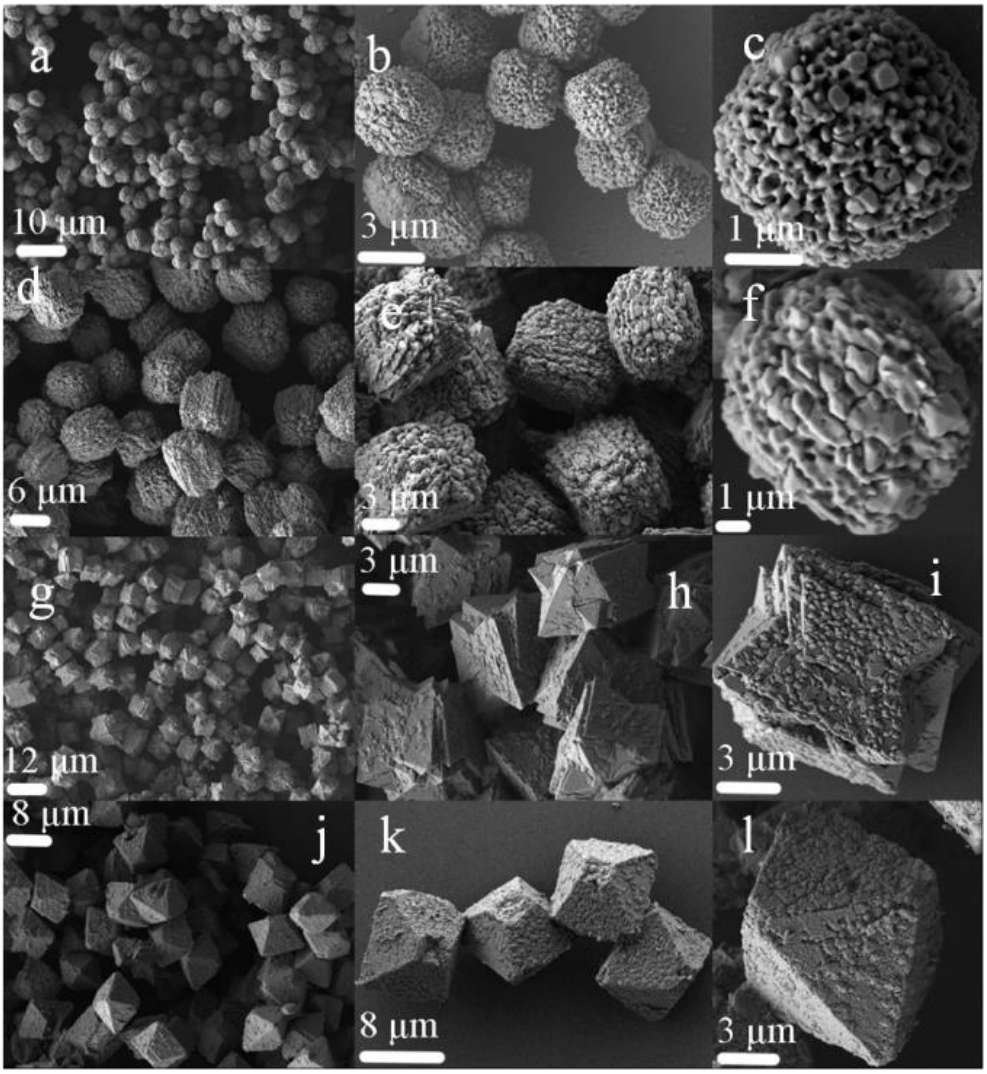

Figure 4. Typical SEM images of $Cu_4O(PO_4)_2$ superstructures (a-c) P1; (d-f) P2; (g-i) P3; (j-l) P4.

The screwy cubic-like morphology can be seen in Fig. 1e, and the size of single particle is about 10-11 μm in Fig. 1f. When we assisted sodium dodecylbenzene sulfonate, 0.050 g, and other conditions were the same as the sample in Fig. 1e–f, and octahedron-like superstructure of $Cu_2(OH)PO_4$ can be seen in Fig. 1g (the product named S4), and the size of single octahedron particle is about 10-11 μm in Fig. 1h. The octahedron crystals have the slippery surfaces. Thus, by using of sodium dodecylbenzene sulfonate, the growth of the $Cu_2(OH)PO_4$ superstructure could be controlled.Fig. 2a (the product named S5) display typical SEM images of the product which was prepared with 0.210 g of $CuSO_4 \cdot 5H_2O$ and 0.210 g of $(NH_4)_2HPO_4$ in a solvent of 10 mL H_2O at 200 ^oC for 24 h. The rod-like morphology can be seen in Fig. 2a, and the size of single particle is about 10-11 μm. When increasing the reaction time to 48 hours, we can obtain double-flower-like superstructure in Fig. 2b (the product named S6). The peanut-like $Cu_2(OH)PO_4$ superstructure was obtained in Fig. 2c (the product named S7), when we assisted sodium dodecylbenzene sulfonate, 0.013 g, and decreasing the amount of $CuSO_4 \cdot 5H_2O$ to 0.124 g. Fig. 2d (the product named S8) display typical SEM images of the product prepared with 0.210 g of $CuSO_4 \cdot 5H_2O$, 0.210 g of $(NH_4)_2HPO_4$ and 0.015 g of sodium dodecylbenzene sulfonate in a solvent of 30 mL H_2O at 200 ^oC for 24 h, dumbbell-shaped $Cu_2(OH)PO_4$ superstructure, and the size of single particle is about 9-10 μm.

From ESI Fig. 4 thermogravimetry analysis of various $Cu_2(OH)PO_4$ superstructures, $Cu_2(OH)PO_4$ decomposed as the increasing temperature in the air, which could maintain stable after 600 ^oC. $Cu_4O(PO_4)_2$ superstructure could be easily obtained by calcining $Cu_2(OH)PO_4$ superstructure at 600 ^oC for 12 hours in the air. XRD patterns of the as-prepared samples are shown in ESI Fig. 5, and one XRD pattern is single list for comparison in ESI Fig. 6. We can see that all peaks of ESI Fig. 6a confirm the product is $Cu_4O(PO_4)_2$ complex (JCPDS No.-310471). Fig. 3 shows a schematic crystal structure of the $Cu_4O(PO_4)_2$ super cell (2×2×2 slabs). Notably, the $Cu_4O(PO_4)_2$ also consisted of CuO5 and CuO6 units. The only difference in structure between $Cu_2(OH)PO_4$ and $Cu_4O(PO_4)_2$ is the OH species attached on Cu sites,[33] which might play an important role for their different physical-chemical properties. Fig. 4 displays typical SEM images of the product prepared with calcining S1-S4 superstructures in the air at 600 ^oC for 12 h.

Fig. 4a-c (the product named P1) displays typical SEM images of porous spheres walnut-like superstructures with sizes of 3-4 μm. The morphology of the precursor S1 is maintained completely. But unlike the precursor S1, there are many nanopores which were caused by the releasing of gas from the single rough sphere walnut-like superstructure. This phenomenon also can be seen in Fig. 4d-f (the product named P2), we also find that there are many nanopores on P2 and the morphology of oblong walnut-like superstructure is maintained. There are many nanoparticles on the surface of screwy cubic-like superstructure which make it roughly, but unlike P1 or P2 there are not any visible pore in Fig. 4g-i (the product named P3). The rough octahedron $Cu_4O(PO_4)_2$ can be easily obtained and the morphology are shown in Fig. 4j-l (the product named P4). The nanoparticle protruded on the surface of P4 as that of P3.

Fig. 5a-b (the product named P5) displays typical SEM images of the rod-like $Cu_4O(PO_4)_2$, the size of which is the same as the precursor S5 with 10-11 μm. As the others, there are many nanoparticles leading the rough surface. The morphology of product in Fig. 5c-d is rough double-flower-like superstructure (the product named P6). The porous peanut-like superstructure is shown in

Fig. 5e (the product named P7), which shows incompact structure in Fig. 5f. The dumbbell-shaped $Cu_4O(PO_4)_2$ superstructure (the product named P8) is also easily obtained after calcing the dumbbell-shaped S8 in Fig. 5g-h. But this superstructure is not rough as other $Cu_4O(PO_4)_2$ superstructures, maybe such dumbbell-shaped superstructure is strong enough to decomposition.

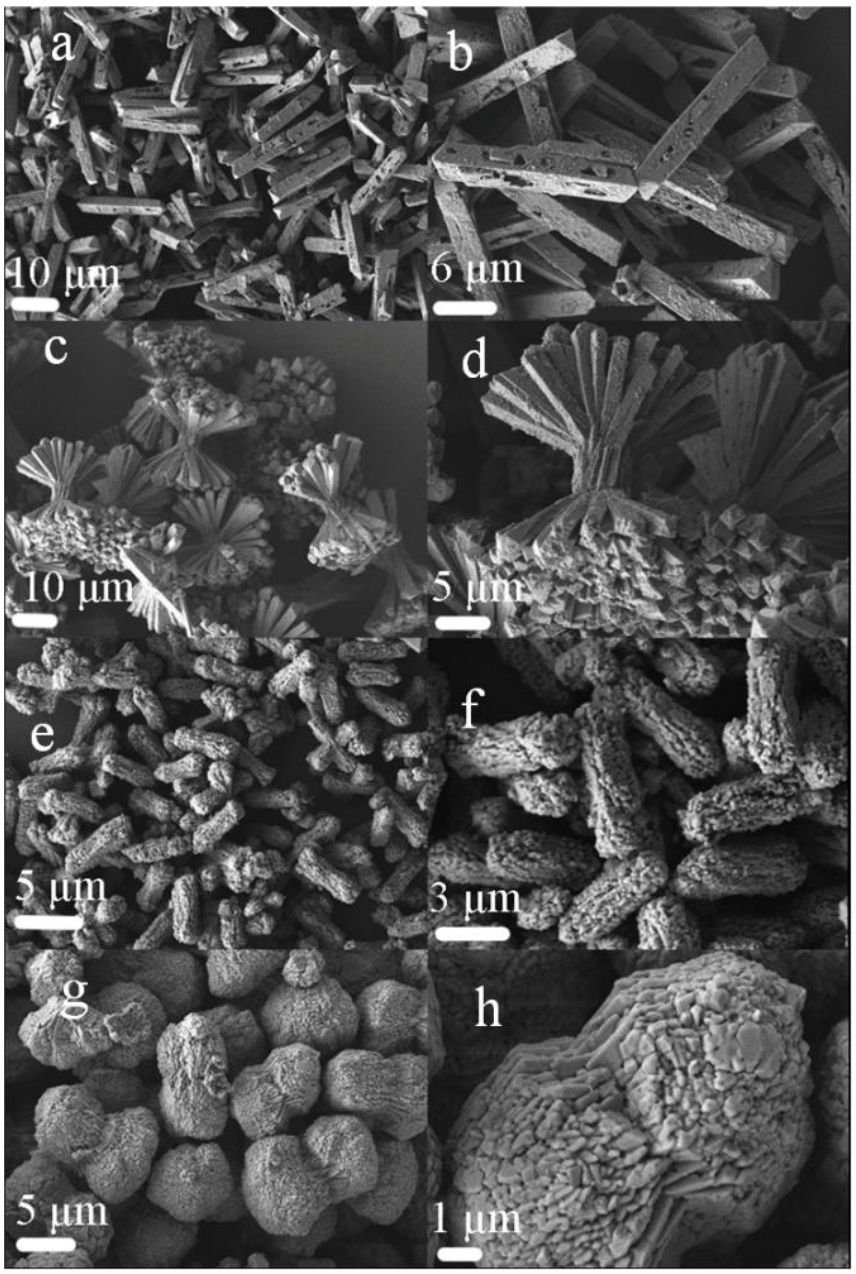

Figure 5. Typical SEM images of $Cu_4O(PO_4)_2$ superstructures (a-b) P5; (c-d) P6; (e-f) P7; (g-h) P8.

Recently, nanomaterials have shown severe cytotoxicity.[51-53] Some studies have revealed that copper based nanomaterials possess high antibacterial activities with minimal perturbation to human cells, which might lead to a range of medical and environmental applications.[30, 54] In this work, the antibacterial activities of $Cu_4O(PO_4)_2$ superstructures were

studied. We evaluated the antibacterial property of $Cu_4O(PO_4)_2$ superstructures for both Gram negative and Gram positive firstly by measuring the microbial viability of bacteria incubated with these superstructures (see antibacterial experimental details).

Table 1. MICs of the synthetic $Cu_4O(PO_4)_2$ superstructures.

Minimum inhibitory concentration/(μg mL^{-1})						
	Gram positive			Gram negative		
No.	*B.subtilis*	*S.aureus*	*S.faecalis*	*P.areuginosa*	*E.cloacae*	*E. coli*
P1	1.562	1.562	1.562	6.25	6.25	3.125
P2	3.125	3.125	1.562	6.25	12.5	6.25
P3	6.25	3.125	3.125	6.25	3.125	12.5
P4	12.5	12.5	12.5	12.5	12.5	6.25
P5	6.25	3.125	3.125	12.5	3.125	6.25
P6	12.5	3.125	6.25	12.5	12.5	6.25
P7	6.25	3.125	6.25	25	25	25
P8	6.25	3.125	6.25	12.5	12.5	25
Penicillin	1.562	1.562	1.562	6.25	3.125	3.125
Kanamycin	0.39	1.562	3.125	3.125	1.562	3.125

The results are presented in Table 1 and verify that all samples have bacteriostatic ability to some of the tested six bacteria: *B. subtilis*, *S. aureus*, *S. faecalis*, *P. aeruginosa*, *E. cloacae* and *E. coli* bacteria. The first three of which are Gram positive and the latter three are Gram negative. Table 1 is MICs of various $Cu_4O(PO_4)_2$ superstructures. From Table 1, it is evident that P1, P2 and P3 have effective antibacterial activities against *P. aeruginosa* which is the same as penicillin, and P1 also kills *E. coli*. effec tive as penicillin. P3 and P5 could kill *E. cloacae* effective as penicillin. From all MICs of all Gram negative bacteria for eight samples, $Cu_4O(PO_4)_2$ superstructures have some selective antibacterial activities. What's more, $Cu_4O(PO_4)_2$ superstructures have effective broad-spectrum antibacterial activities against Gram positive bacteria except P4 and P6. P1 has the most effective antibacterial activities against Gram positive bacteria of all, and its MICs of all Gram negative bacteria are 1.562, 1.562 and 1.562, respectively. More importantly, this effect is the same as that of penicillin. These results might be reasonable in those materials with different morphologies having different surface conditions. From ESI Table 1, Brunauer-Emmett-Teller (BET) measurements of the synthetic $Cu_2(OH)PO_4$ and $Cu_4O(PO_4)_2$ superstructures were also tested to gain further insight into the material structure. We found that BET surface areas of all the superstructures were not very large. But the P1 has the largest value among $Cu_4O(PO_4)_2$ superstructures, and from SEM image Fig.4 a-c there are many nanopores in the single rough sphere walnut superstructure which make effective contact with bacteria and cause good antibacterial activities. The different surface-interface characters might have different chemical-physical adsorption-desorption abilities towards the bacteria, resulting in different antibacterial activities.

4. CONCLUSION

In summary, we have successfully synthesized various morphologies of $Cu_4O(PO_4)_2$ superstructures which was obtained by calcining the $Cu_2(OH)PO_4$ superstructure. The primarily measurement of antibacterial activities for $Cu_4O(PO_4)_2$ indicates that these materials are a kind of good inorganic antibacterial agents. More importantly, different morphologies of $Cu_4O(PO_4)_2$ superstructure show different antibacterial properties, which helps antibacterial material researcher to find a good example for morphology dependent antibacterial properties. There are many nanocrystal structures on the $Cu_4O(PO_4)_2$ superstructures which might make effective contact with bacteria. But the scientific and accurate reason for different antibacterial activities between different $Cu_4O(PO_4)_2$ superstructures is need to further research. Furthermore, this work is a good example to prove physical-chemical properties dependent on material morphologies, which encourages scientists to control the morphology of materials precisely to control their performance.

ACKNOWLEDGMENT

This work is supported by the National Natural Science Foundation of China (21201010, 51272168, 21071006), Science & Technology Foundation of Henan Province (122102210253) and Project of Science & Technology of Anyang city.

Supporting Information:

Electronic Supplementary Information (ESI) available: [Crystal structure of the $Cu_2(OH)PO_4$ super cell (2×2×2 slabs); XRD patterns of $Cu_2(OH)PO_4$ $Cu_4O(PO_4)_2$ superstructures; Thermogravimetry analysis of various $Cu_2(OH)PO_4$ superstructures; BET surface areas of the synthetic $Cu_2(OH)PO_4$ and $Cu_4O(PO_4)_2$ superstructures.]

References

1. C. Burda, X. B. Chen, R. Narayanan and M. A. El-Sayed, *Chem. Rev.*, 105 (2005) 1025.
2. X. Duan, Y. Huang, Y. Cui, J. Wang and C. M. Lieber, *Nature*, 409 (2001) 66.
3. A. M. Cao, J. S. Hu, H. P. Liang and L. J. Wan, *Angew. Chem. Int. Ed.*, 44 (2005) 4391.
4. A. Nishino, *J. Power Sources*, 60 (1996) 137.
5. S. Niwa, Y. Taketani, *J. Power Sources*, 60 (1996) 165.
6. H. Pang, Y. Ma, G. Li, J. Chen, J. Zhang, H. Zheng and W. Du, *Dalton Trans.*, 41 (2012) 13284-13291.
7. H. Pang, Z. Yan, W. Wang, J. Chen, J. Zhang and H. Zheng, *Nanoscale*, 4 (2012) 5946-5953.
8. H. Pang, J. Deng, J. Du, S. Li, J. Li, Y. Ma, J. Zhang and J. Chen, *Dalton Trans.*, 41 (2012) 10175-10181.
9. Y. Cai, H. Pan, X. Xu, Q. Hu, L. Li and R. Tang, *Chem. Mater.*, 19 (2007) 3081.
10. D. F. Zhang, L. D. Sun, G. Xu and C. H. Yan, *Phys. Chem. Chem. Phys.* , 8 (2006) 4874.
11. F. Favier, E. C. Walter, M. P. Zach, T. Benter and R. M. Penner, *Science*, 293 (2001) 2227.
12. T. Zhang, W. Dong, M. Keeter-Brewer, K. Sanjit, R. N. Njabon and Z. R. Tian, *J. Am. Chem. Soc.*, 128 (2006) 10960.
13. S. H. Yu and M. Yoshimura, *Adv. Mater.*, 14 (2002) 296.
14. C. Wu, Y. Xie, D. Wang, J. Yang and T. Li, *J. Phys. Chem. B*, 107 (2003) 13583.
15. H. Pang, Q. Y. Lu, C. Y. Chen, X. R. Liu and F. Gao, *J. Mater. Chem.*, 21 (2011) 13889-13894.

16. H. Pang, F. Gao and Q. Y. Lu, *Chem. Commun.*, 2009, 1076-1078.
17. S. Ray, R. Mohan, J. K. Singh, M. K. Samantaray, M. M. Shaikh, D. Panda, P. Ghosh, *J. Am. Chem. Soc.*, 129 (2007) 15042–15053.
18. L. K. Adams, D. Y. Lyon, P. J. Alvarez, *Water Res.*, 40 (2006) 3527 -3532.
19. K. Kasemets, A. Ivask, H. C. Dubourguier and A. Kahru, *Toxicol. In Vitro*, 23 (2009) 1116–1122.
20. V. Aruoja, H. C. Dubourguier, K. Kasemets and A. Kahru, *Sci. Total Environ*., 400 (2009) 1461–1468.
21. X. Peng, L. Manna, W. Yang, J. Wickham, E. Scher, A. Kadavanich and A. P. Alivisatos, *Nature*, 404 (2000) 59–61.
22. M. A. El-Sayed, *Acc. Chem. Res.*, 34 (2001) 257–264.
23. S. H. Jiao, L. F. Xu, K. Jiang, D. S. Xu, *Adv. Mater.*, 18 (2006) 1174–1177.
24. H. Q. Cao, G. Z. Wang, S. C. Zhang, X. R. Zhang and D. Rabinovich, *Inorg. Chem.*, 45 (2006) 5103–5108.
25. H. Li, R. Liu, R. X. Zhao, Y. F. Zheng, W. X. Chen and Z. D. Xu, *Cryst. Growth Des.*, 6 (2006) 2795– 2798.
26. H. Pang, B. Zhang, J. M. Du, J. Chen, J. S. Zhang and S. J. Li, *RSC Adv.*, 2 (2012) 2257–2261.
27. H. Pang, Q. Y. Lu and F. Gao, *Chem. Commun.*, 47 (2011) 11772-11774
28. H. Pang, Q. Y. Lu, J. J. Wang, Y. C. Li and F. Gao, *Chem. Commun.*, 46 (2010) 2010-2012.
29. H. Pang, F. Gao and Q. Y. Lu, *CrystEngChem*, 12 (2010) 406-411.
30. H. Pang, Q. Y. Lu, Y. C. Li and F. Gao, *Chem. Commun.*, 2009, 7542-7544.
31. J. J. Chiu, W. S. Wang, C. C. Kei, C. P. Cho, T. P. Perng, P. K. Wei and S. Y. Chiu, *Appl. Phys. Lett.*, 83 (2003) 4607-4609.
32. J. J. Chiu, C. C. Kei, T. P. Perng and W. S. Wang, *Adv. Mater.*, 15 (2003) 1361–1364.
33. Y. S. Zhao, C. A. Di, W. S. Yang, G. Yu, Y. Q. Liu and J. N. Yao, *Adv. Funct. Mater.*, 16 (2006) 1985– 1991.
34. J. S. Hu, H. X. Ji, A. M. Cao, Z. X. Huang, Y. Zhang, L. J. Wan, A. D. Xia, D. P. Yu, X. M. Meng and S. T. Lee, *Chem. Commun.*, 2007, 3083 -3085.
35. D. Xu, D. Xue, H. Ratajczak, *J. Mol. Struct.*, 740 (2005) 37-45. (b) D. Xu and D. Xue, *Physica B* 2005, 370, 84–89. (c) D. Xu and D. Xue, *J. Cryst.Growth*, 286 (2006) 108–113.
36. A. Clearfield, *Curr. Opin. Solid State Mater. Sci.*, 1 (1996) 268–278. (b) M. K. Cerreta and K. A. Berglund, *J. Cryst. Growth*, 84 (1987) 577–588.
37. D. Kong, Y. Li, X. Ouyang, A. V. Prosvirin, H. Zhao, J. H. Jr. Ross, K. R. Dunbar and A. Clearfield, *Chem. Mater*., 16 (2004) 3020–3031. (b) R. L. Frost, T. Kloprogge, P. A. Williams, W. Martens, T. E. Johnson and P. Leverett, *Spectrochim. Acta A*, 58 (2002) 2861–2868.
38. (a) J. Yang, L. Qi, C. Lu, J. Ma and H. Cheng, *Angew. Chem. Int.Ed.*, 44 (2005) 598–603. (b) A. A. Belik, M. Azuma and M. Takano, *J. Solid. State Chem.*, 177 (2004) 883–888. (c) B. I. Lazoryak, N. Khan, V. A. Morozov, A. A. Belik and S. S. Khasanov, *J. Solid State Chem.*, 145 (1999) 345–355.
39. J. B. Anderson, G. L. Shoemaker and E. Kostiner, *J. Solid*. *State Chem.*, 24 (1978) 49–57.
40. M. Brunel-LauÈgt, A. Durif and J. T.Guitel, *J. Solid. State. Chem.*, 25 (1978) 39-47.
41. H. M. Schwunck, P. Moser and W. Jung, *Z. anorg. allg. Chem.*, 624 (1998) 1262-1266.
42. X. J. Meng, K. F. Lin, X. Y. Yang, Z. H. Sun, D. Z. Jiang and F. S. Xiao, *J. Catal.*, 218 (2003) 460–464.
43. http://www.mindat.org/min-2394.html (Accessed January, 2008).
44. A. Cordsen, *Can. Mineral.*, 16 (1978) 153-157.
45. F. S. Xiao, J. Sun, X. Meng, R. Yu, H. Yuan, D. Jiang, S. Qiu and R. Xu, *Appl. Catal. A*, 207 (2001) 267-271.
46. A. A. Belik, H. J. Koo, M. H. Whangbo, N. Tsujii, P. Naumov and E. T. Muromachi, *Inorg. Chem.*, 46 (2007) 8684–8689.
47. S. N. Reddy, R. V. S. S. N. R. Kumer, B. J. Reddy and P. S. Rao, *Ferroelectrics*, 166 (1995) 55-62.

48. F. S. Xiao, J. Sun, X. Meng, R. Yu, H. Yuan, J. Xu, T. Song, D. Jiang and R. Xu, *J. Catal.*, 199 (2001) 273–281.
49. X. Meng, K. Lin, J. Sun, M. Yang, D. Jiang and F. S. Xiao, *Catal. Lett.*, 76 (2001) 241.
50. J. Xu and D. Xue, *J. Phys. Chem. B*, 110 (2006) 7750–7756.
51. Y. Su, Y. He, H. Lu, L. Sai, Q. Li, W. Li, L. Wang, P. Shen, Q. Huang and C. Fan, *Biomaterials*, 30 (2009) 19–25.
52. Y. Su, M. Hu, C. Fan, Y. He, Q. Li, W. Li, L. Wang, P. Shen and Q. Huang, *Biomaterials*, 31 (2010) 4829–4834.
53. W. Hu, C. Peng, W. Luo, M. Lv, X. Li, D. Li, Q. Huang and C. Fan, *ACS Nano*, 4 (2010) 4317–4323.
54. F. Gao, H. Pang, S. P. Xu, and Q. Y. Lu, *Chem. Commun.*, 2009, 3571–3573.

Electronic Supplementary Information (ESI)

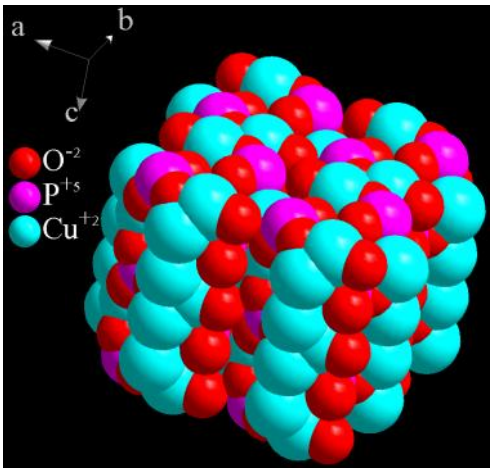

ESI Fig. 1 crystal structure of the $Cu_2(OH)PO_4$ super cell (2×2×2 slabs).

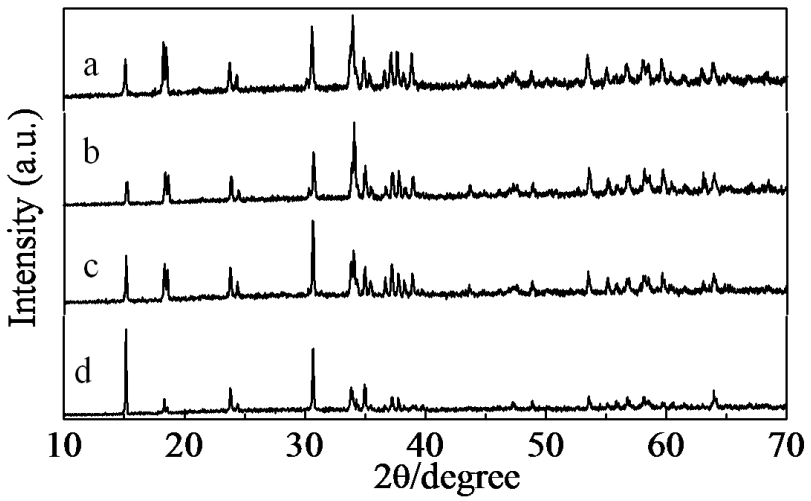

ESI Fig. 2 XRD patterns of $Cu_2(OH)PO_4$ superstructures (a) S1; (b) S2; (c) S3; (d) S4.

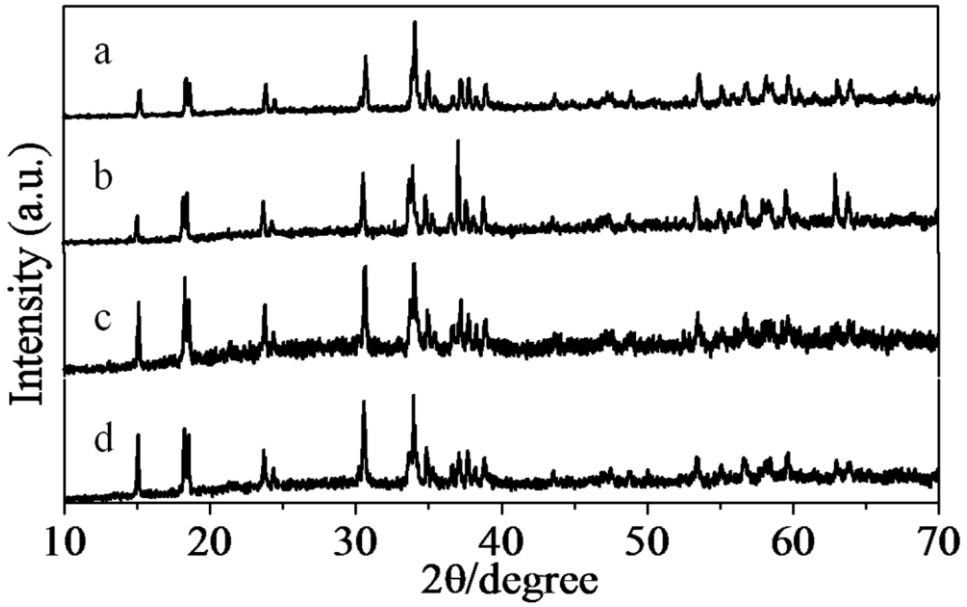

ESI Fig. 3 XRD patterns of $Cu_2(OH)PO_4$ superstructures (a) S5; (b) S6; (c) S7; (d) S8.

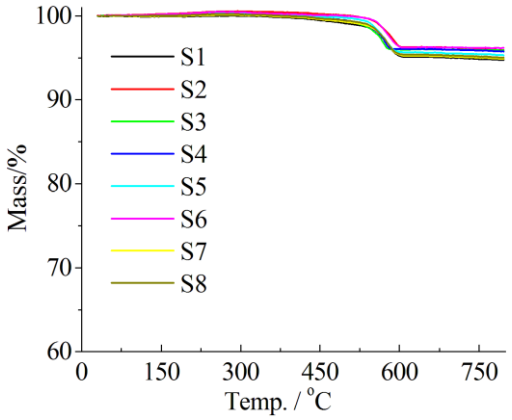

ESI Fig. 4 Thermogravimetry analysis of various $Cu_2(OH)PO_4$ superstructures.

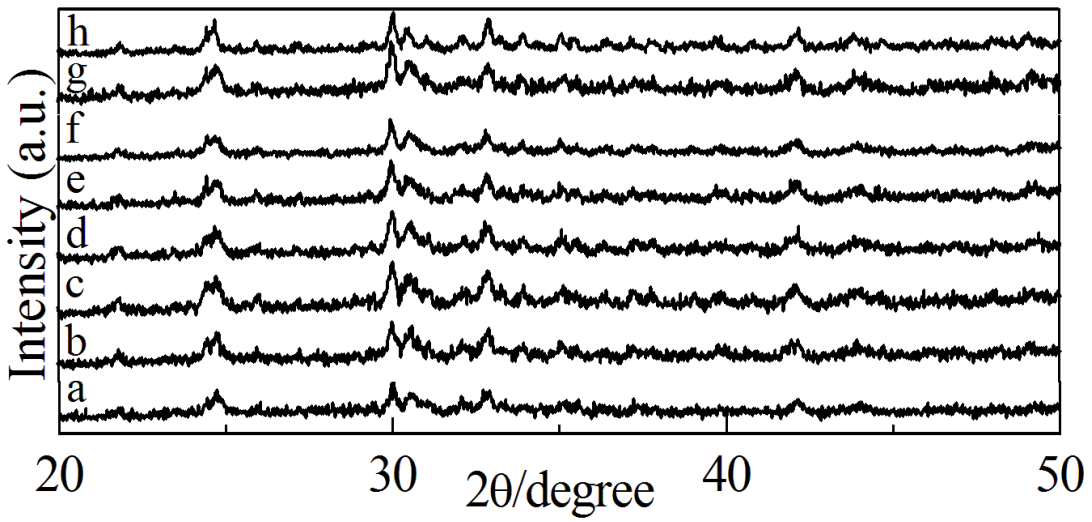

ESI Fig. 5 XRD patterns of $Cu_4O(PO_4)_2$ superstructures (a) P1; (b) P2; (c) P3; (d) P4; (e) P5; (f) P6; (g) P7; (h) P8.

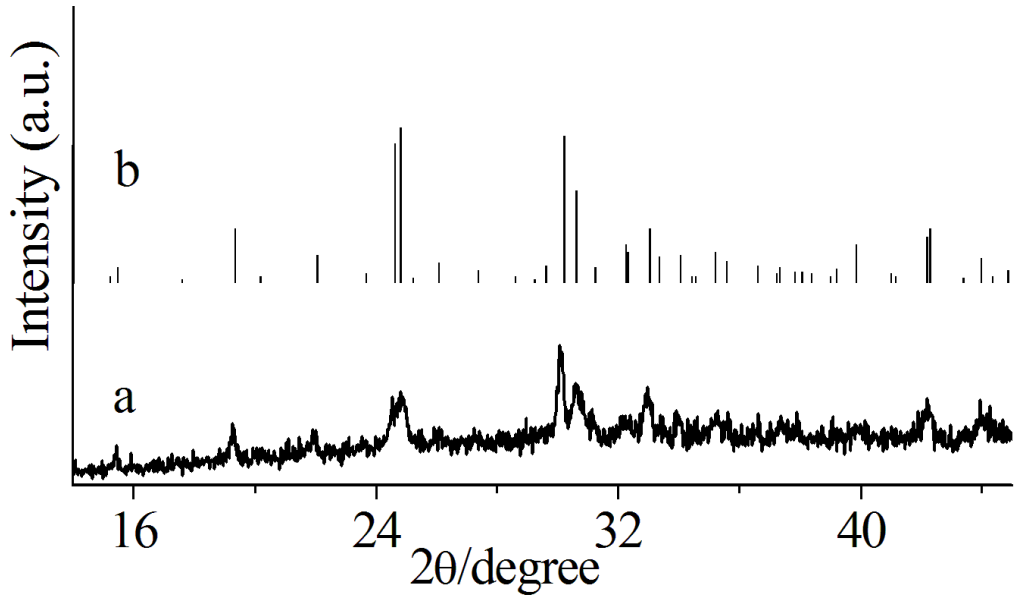

ESI Fig. 6 XRD patterns of the $Cu_4O(PO_4)_2$ superstructures (a) P1; (b) JCPDS No.-310471.

Sample NO.	The BET surface areas / m^2 g^{-1}
S1	8.6
S2	7.2
S3	6.3
S4	5.4
S5	3.2
S6	3.2
S7	3.6
S8	3.4
P1	13.6
P2	12.2
P3	12.4
P4	12.3
P5	8.6
P6	8.1
P7	8.2
P8	7.8

ESI Table 1 BET surface areas of the synthetic $Cu_2(OH)PO_4$ and $Cu_4O(PO_4)_2$ superstructures.